Interaction of two parallel femtosecond filaments at different wavelengths in air

Jian Wu, Yuqi Tong, Xuan Yang, Hua Cai, Peifen Lu, Haifeng Pan, and Heping Zeng*

State Key Laboratory of Precision Spectroscopy, East China Normal University, Shanghai 200062, China
**Corresponding author: hpzeng@phy.ecnu.edu.cn*

Received July 16, 2009; revised September 18, 2009; accepted September 18, 2009;
posted September 24, 2009 (Doc. ID 114024); published October 13, 2009

We study the interaction of two parallel-launched femtosecond filaments at their fundamental-wave and second-harmonic frequencies in air. Besides the Kerr effect within the pulse duration, the impulsive alignment of the diatomic molecules in the fundamental-wave filament leads to controllable and field-free achievable attraction, fusion, or repulsion of the second-harmonic filament. The molecular-alignment-assisted filament interaction is further confirmed by the fluorescence intensity variation and spectral modulation of the second-harmonic filament at various molecular alignment revivals. © 2009 Optical Society of America

OCIS codes: 320.7110, 260.5950, 020.2649.

Self-guided light filaments in transparent nonlinear optical media have been extensively studied for important applications in various fields [1]. It is highly desired to precisely control filament dynamics and sequential nonlinear optical processes, which can be achieved through interaction between intense filaments and have been demonstrated [2–6] when they were temporally synchronized. The plasma channel was recently shown to be revivable by detaching the weakly bound electrons [7]. For molecular gases, the relative orientation of the molecules to the field polarization provides an additional degree of freedom to control the pulse propagation. Molecular alignment revives periodically after the impulsive excitation and thus can be used to get field-free control of filament interactions. The impulsive molecular alignment has been demonstrated to be efficient in modulating pulse spectra [8,9] and polarization [10], controlling the filament length and pulse self-compression [11,12] and supercontinuum generation [13], enhancing or destructing filamentation [14–17], and manipulating nonlinear couplings of noncollinearly crossed filaments [18].

In this Letter, we experimentally demonstrate that impulsive molecular alignment could enforce interaction of spatially separated parallel filaments at different wavelengths, resulting in controllable attraction, repulsion, and fusion of filaments. We investigate the filament interaction by directly observing the transverse displacements during the intense filamentation, which is also confirmed by the fluorescence intensity variation and spectral modulation of the filaments. Furthermore, we show that the Kerr effect within the pulse duration can be clearly distinguished from the time-delayed response of the molecular alignment, featuring different filament interactions.

Figure 1(a) schematically shows our experimental setup, where an output from an amplified Ti:sapphire laser system (50 fs/800 nm/1 kHz) was used. A beta-barium borate crystal (Type I, 200 μm thick) was used to generate a second-harmonic (SH) beam. The fundamental-wave (FW) and SH beams were respectively focused with a concave mirror and a convex lens (f=100 cm) and then recombined with a dichromatic mirror to generate two parallel filaments (with an initial separation of ~100 μm) in air. The positive delays account for the FW ahead of the SH pulse. The FW and SH pulses after the combining mirror were measured to be ~1.02 and 0.25 mJ per pulse, respectively, leading to two single filaments of ~6.5 and 14.0 cm in length. By adjusting the relative position of the focusing lens in the SH arm, the center part of the SH filament was controlled at almost the same position of the FW one along the propagation direction. The filament interaction was checked by collecting the ionization-induced fluorescence of the FW and SH filaments (around the center parts) with a microscope objective (MO, 10×) and then recorded with a monochrome digital CCD. The inset of Fig. 1(a) shows the typical fluorescence image of the parallel filaments, where the bright (lower) one accounts for the FW filament and the other one is the SH. As compared with the imaging of the beam profiles at the end of the filaments in [14–18], here the attrac-

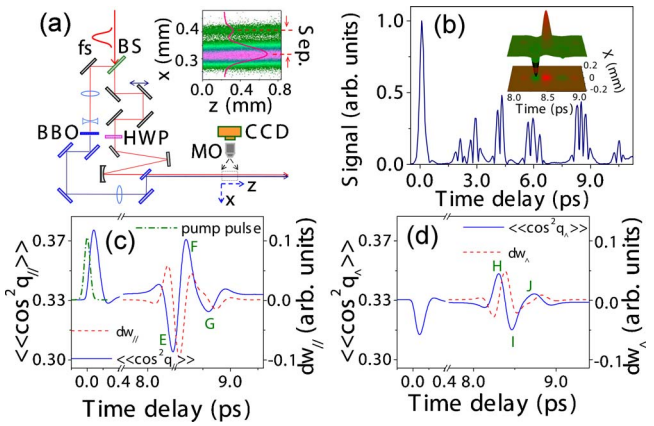

Fig. 1. (Color online) (a) Schematic of our experimental setup (inset, the fluorescence image of the filaments); (b) measured and (c), (d) calculated molecular alignment signal of air along the direction parallel (c) or perpendicular (d) to the field polarization. The induced frequency shifts and excitation pulse envelope are shown as dashed and dash–dotted curves, respectively. The inset of (b) shows a 2D distribution of the refractive index change.

tion and the repulsion of the parallel filaments were characterized by directly checking the spatial separations between the filament cores, as indicated in Fig. 1(a), with the transverse images of the fluorescence inside the intense filaments. Here, the systematic fluctuations of the separation and fluorescence measurements were estimated to be $\sim\pm5\%$ and $\sim\pm4\%$, respectively.

The diatomic molecules of N_2 and O_2 in air were prealigned by the FW filament through the impulsive rotational Raman excitation. Figure 1(b) shows the measured molecular alignment signal of air $\sim(\langle\langle\cos^2\theta_{\parallel}\rangle\rangle-1/3)^2$ by using the weak-field polarization technique [19]. The calculated metrics $\langle\langle\cos^2\theta_{\parallel}\rangle\rangle$ and $\langle\langle\cos^2\theta_{\perp}\rangle\rangle=(1-\langle\langle\cos^2\theta_{\parallel}\rangle\rangle)/2$ are correspondingly shown in Figs. 1(c) and 1(d). The refractive index is relatively increased or decreased as $\delta n_{\mathrm{mol}}(r,t)=2\pi(\rho_0\Delta\alpha/n_0)(\langle\langle\cos^2\theta\rangle\rangle(r,t)-1/3)+\delta n_{rR}(r,t)$ [12], depending on whether the molecular orientation is parallel ($\langle\langle\cos^2\theta\rangle\rangle>1/3$) or perpendicular ($\langle\langle\cos^2\theta\rangle\rangle<1/3$) to the field polarization. Since the molecular alignment degree (proportional to the FW intensity) decreases along the transverse distance from the FW filament core, the parallel-launched SH filament experiences a gradual change of the refractive index along the transverse direction. As an example, the inset of Fig. 1(b) shows a 2D distribution of the refractive index change induced by a FW filament around the revival time from 8.0 to 9.0 ps. The prealigned molecules excited by the FW filament therefore set a uphill or downhill refractive index potential for the parallel-launched SH filament. The SH filament is attracted close to the FW one when it is tuned to the parallel revival of the molecular alignment with an uphill refractive index potential created by the FW filament wake. In contrast, filament repulsion is expected for the perpendicular molecular alignment revival.

Figure 2(a) shows the measured time-dependent filament separations around the zero time delay. The filaments were mutually attracted with a decreased separation as they temporally approached. Furthermore, filament fusion was observed around delay A, as shown in the inset of Fig. 2(a) of the measured fluorescence image. This filament attraction and fusion within the pulse duration originated mainly from the Kerr response of air [4], which increased the local refractive index through the self- and cross-phase modulation of the FW and SH beams. As we can notice from Fig. 2(a), comparing to the negative side of the time delay, there is a broader range on the positive side to ensure the filament attraction and fusion. This was caused by the parallel-aligned molecules in air created by the FW filament, which featured with a certain delay (about $\sim$100 fs) with respect to the FW pulse excitation [as revealed in Fig. 1(c)] and hence broadened the time range of the interaction. For the negative delays, the low intensity of the SH beam was insufficient to ensure the filament attraction through molecular alignment. The change of the filament separation originated mainly from the movement of the SH filament affected by the FW one. At different delays, the SH filament was

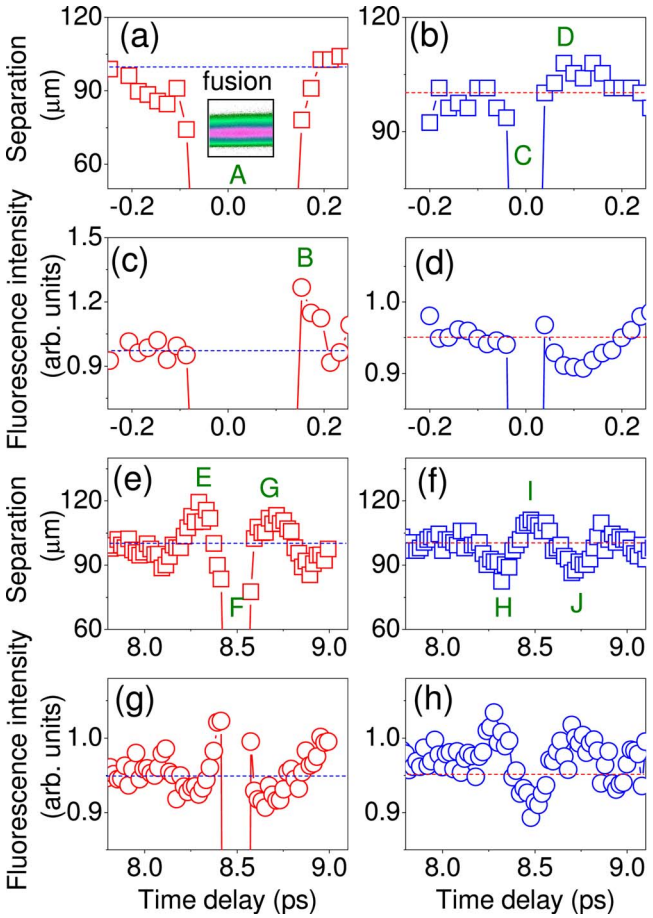

Fig. 2. (Color online) Measured displacement and fluorescence intensity of the SH filament versus its time delay with respect to the FW pulse. The polarization of the FW filament is parallel (left column) and perpendicular (right column) to the SH filament. The dashed lines mark the average filament separation and fluorescence intensity.

repulsed away or attracted close to the FW one or even fused into the FW filament, which then returned to its original position when it was out of the interaction range. Since the electron in a parallel-oriented molecule is easier to free than that in a perpendicularly oriented one [20], as shown in Fig. 2(c), a relative large fluorescence intensity around delay B was observed that was consistent with the filament attraction by parallel molecular alignment shown in Fig. 2(a).

Figures 2(b) and 2(d) show the measured displacement and fluorescence intensity of the SH filament when the FW polarization was orthogonal to the SH one. Owing to the reduced Kerr effect induced by cross-phase modulation between the orthogonally polarized beams ($n_{2,\parallel}^{\mathrm{XPM}}=3n_{2,\perp}^{\mathrm{XPM}}$), the filament attraction and fusion were observed in a short time range around the zero delay within the pulse duration (delay C), which differed from the collinear case as observed in [15,16]. This difference might originate from different experimental scheme and laser parameters, which caused different Kerr and plasma effects experienced by the probe beam. The response of the molecular alignment was $\sim$100 fs delayed with respect to the pump-pulse excitation. Therefore repulsion of the SH filament was observed at delay D as

indicated in Fig. 2(b), corresponding to the perpendicularly aligned molecules by the orthogonally polarized FW pulse [Fig. 1(d)]. As shown in Fig. 2(d), the fluorescence intensity of the SH filament decreased at delay D owing to the relatively small ionization probability of the perpendicularly oriented molecules.

By tuning the SH pulse to the field-free revivals of the prealigned molecules, controllable attraction and repulsion of the SH filament could also be observed. As shown in Figs. 1(c) and 1(d), for a delay range from 8.0 to 9.0 ps including the full revival of N_2 and three-quarter revival of O_2, the molecules were reoriented perpendicular or parallel to the SH polarization at delays E, G, and I or F, H, and J, respectively. The SH filament was therefore displaced with increased or decreased separations from the FW when it was properly tuned to match the perpendicular or parallel molecular alignment revivals, as observed in Figs. 2(e) and 2(f). Since $|\langle\langle\cos^2\theta_\perp\rangle\rangle| < |\langle\langle\cos^2\theta_\parallel\rangle\rangle|$ as indicated in Figs. 1(c) and 1(d), the filament displacing was relatively smaller for the case of orthogonally polarized FW and SH beams [Fig. 2(f)] than the case of parallel polarizations [Fig. 2(e)]. Only filament fusion was observed at delay F for parallel polarizations rather than the limited attraction at delays H and J for orthogonal polarizations. As shown in Figs. 2(g) and 2(h), the ionization-induced fluorescence of the SH filament was correspondingly modulated by following the molecular alignment revivals owing to the orientation-dependent ionization probability [20].

The time-dependent molecular alignment revival also induced an additional spectral modulation to the SH pulse as [8,9] $\delta\omega(t) \propto -\partial/\partial t(\langle\langle\cos^2\theta\rangle\rangle - 1/3)$. As shown in Fig. 3, the spectrum of the SH filament was blueshifted or redshifted for the falling or rising edges of the molecular alignment revivals as indicated in Figs. 1(c) and 1(d) (dashed curves). It further confirmed that the molecular alignment created by the FW filament acted as the basic mechanism to controllably displace the SH filament.

In summary, we have shown that the parallel-launched SH filament can be attracted, repulsed, or fused by the FW filament in a controllable manner by properly matching it to the revivals of the prealigned molecules in air. When they were temporally synchronized, the Kerr effect of the molecular gas participated in the filament interaction, leading to filament attraction and fusion. This provides us with a flexible field-free approach to precisely control the intense ultrashort filaments.

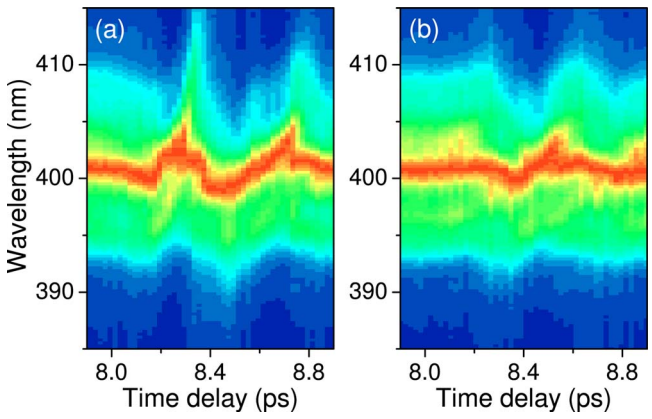

Fig. 3. (Color online) Spectral modulation of the SH filament as a function of the time delay, where the polarization of the FW filament is (a) parallel or (b) perpendicular to the SH filament.

This work was funded in part by National Natural Science Fund (NSFC) (10525416 and 10804032), National Key Project for Basic Research (2006CB806005), Projects from Shanghai Science and Technology Commission (08ZR1407100 and 09QA1402000), and Shanghai Educational Development Foundation (2008CG29).

References

1. A. Couairon and A. Mysyrowicz, Phys. Rep. **441**, 47 (2007).
2. S. Tzortzakis, G. Méchain, G. Patalano, M. Franco, B. Prade, and A. Mysyrowicz, Appl. Phys. B **76**, 609 (2003).
3. A. Couairon, G. Méchain, S. Tzortzakis, M. Franco, B. Lamouroux, B. Prade, and A. Mysyrowicz, Opt. Commun. **225**, 177 (2003).
4. T. Xi, X. Lu, and J. Zhang, Phys. Rev. Lett. **96**, 025003 (2006).
5. P. Béjot, J. Kasparian, and J. P. Wolf, Phys. Rev. A **78**, 043804 (2008).
6. Y. Ma, X. Lu, T. Xi, Q. Gong, and J. Zhang, Appl. Phys. B **93**, 463 (2008).
7. B. Zhou, S. Akturk, B. Prade, Y. André, A. Houard, Y. Liu, M. Franco, C. D'Amico, E. Salmon, Z. Hao, N. Lascoux, and A. Mysyrowicz, Opt. Express **17**, 11450 (2009).
8. J. Ripoche, G. Grillon, B. Prade, M. Franco, E. Nibbering, R. Lange, and A. Mysyrowicz, Opt. Commun. **135**, 310 (1997).
9. H. Cai, J. Wu, A. Couairon, and H. Zeng, Opt. Lett. **34**, 827 (2009).
10. Y. Chen, C. Marceau, F. Théberge, M. Chateauneuf, J. Dubois, and S. L. Chin, Opt. Lett. **33**, 2731 (2008).
11. R. Bartels, T. Weinacht, N. Wagner, M. Baertschy, C. Greene, M. Murnane, and H. Kapteyn, Phys. Rev. Lett. **88**, 013903 (2001).
12. J. Wu, H. Cai, H. Zeng, and A. Couairon, Opt. Lett. **33**, 2593 (2008).
13. J. Wu, H. Cai, Y. Peng, and H. Zeng, Phys. Rev. A **79**, 041404(R) (2009).
14. F. Calegari, C. Vozzi, S. Gasilov, E. Benedetti, G. Sansone, M. Nisoli, S. De Silvestri, and S. Stagira, Phys. Rev. Lett. **100**, 123006 (2008).
15. S. Varma, Y.-H. Chen, and H. M. Milchberg, Phys. Rev. Lett. **101**, 205001 (2008).
16. S. Varma, Y.-H. Chen, and H. M. Milchberg, Phys. Plasmas **16**, 056702 (2009).
17. F. Calegari, C. Vozzi, and S. Stagira, Phys. Rev. A **79**, 023827 (2009).
18. A. C. Bernstein, M. McCormick, G. M. Dyer, J. C. Sanders, and T. Ditmire, Phys. Rev. Lett. **102**, 123902 (2009).
19. V. Renard, M. Renard, S. Guérin, Y. T. Pashayan, B. Lavorel, O. Faucher, and H. R. Jauslin, Phys. Rev. Lett. **90**, 153601 (2003).
20. T. Kanai, S. Minemoto, and H. Sakai, Nature **435**, 470 (2005).